Novel Aqueous Li^+ (or Na^+)/Br^- Hybrid-ion Battery with Super High Areal Capacity and Energy Density

Huaiqing Wang[a b], Renhe Wang[d], Zihan Song[a b], Huamin Zhang[a c], Hongzhang Zhang[a, c] , Yonggang Wang[*d], Xianfeng Li[* a c]

Synthesis of NTP@C nano-composite

The NTP@C nano-composite was synthesized by a modified sol-gel method. Citric acid (0.01 mol) and orthophosphoric acid (0.015 mol, H_3PO_4 85 wt. %) were orderly dissolved into 50 mL absolute ethyl alcohol, after being stirred for 0.5 h at room temperature, tetra-n-butyl titanate (0.01 mol, TBT) was drop-wise added into above mentioned solution. Then the homogeneous gel was formed by the hydrolysis of TBT. The citric used here worked as the chelating agent and carbon source for the in-situ carbon coating. Then the gel was dried at 80 ^oC in water bath, the obtained dry gel was ground with sodium acetate (0.005 mol, CH_3COONa) and heated in a tube furnace at 350 ^oC for 4 h under a flowing Ar atmosphere. The collected power was reground and calcinated at 750 ^oC for 15 h with a ramping rate of 5 ^oC min^{-1} under a flowing Ar atmosphere to obtain the final samples.

Three electrode tests of NTP@C nano-composite and Br^- containing catholyte

In NTP@C half-cell test, the working electrode was prepared by blading coating a homogeneous slurry consisted of NTP@C (active material), Super P (conductive agent) and polyvinylidene fluoride (PVDF, binder) with a mass ratio of 7:2:1 onto the thin carbon paper. The mass loading is as high as 7-10 mg cm^{-2}, which is which is similar with the features of common ion intercalation electrodes in literatures. The saturated calomel electrode (SCE, 0.244V vs. SHE) was used as reference electrode, graphite plate was used as counter electrode. The electrolyte is 2 M Li_2SO_4 and 2 M Na_2SO_4 aqueous solution, respectively.

In the catholyte half-cell tests, the thin carbon paper (1cm*1cm) was used as working voltage. The saturated calomel electrode (SCE, 0.244V vs. SHE) was used as reference electrode, graphite plate was used as counter electrode. The catholyte for charging/discharging tests is a mixed aqueous solution of 0.5 M Li_2SO_4, 0.5 M LiBr, 0.5 M K_2SO_4 or a mixed aqueous solution of 0.5 M Li_2SO_4, 0.5 M LiBr, 0.5 M K_2SO_4, 0.5 M MEP. The cut-off charging capacity is 1 mA h. For the CV tests, 0.05 mM Br_2 was generated by charging above catholytes.

Calculation of the ion conductivity by CV

The diffusion coefficient is calculated by the CV response using the Randles-Sevick equation:

$$Ip = 0.4463(F^3/RT)^{1/2}n^{3/2}AD^{1/2}Cv^{1/2} = 2.69 \times 10^5 n^{3/2}AD^{1/2}Cv^{1/2}$$

n is the number of electrons transferred in the redox process, A is the electrode area, F is the Faraday constant, D is diffusion coefficient and C is the concentration of Br_3^- or alkaline metal ion.

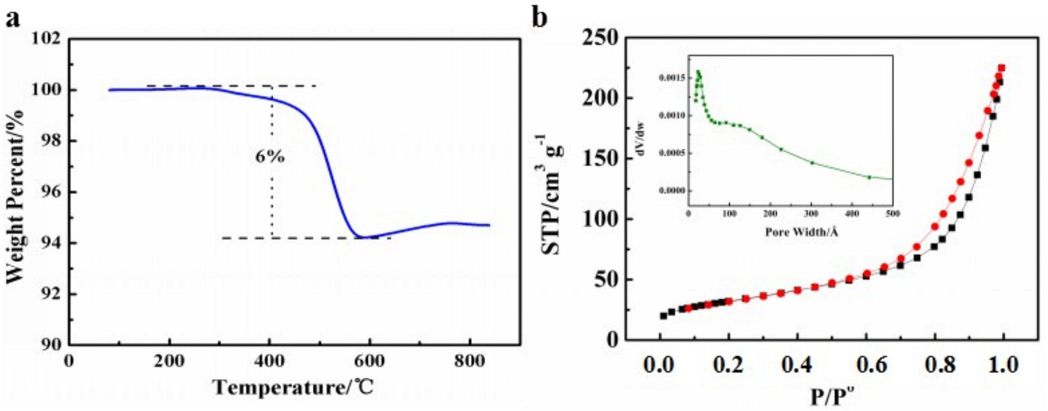

Figure S1. Physical characterization of as-prepared NTP@C particles: (a) TGA profile of as-prepared NTP@C; (b) Nitrogen adsorption−desorption isotherm of as-prepared NTP@C.

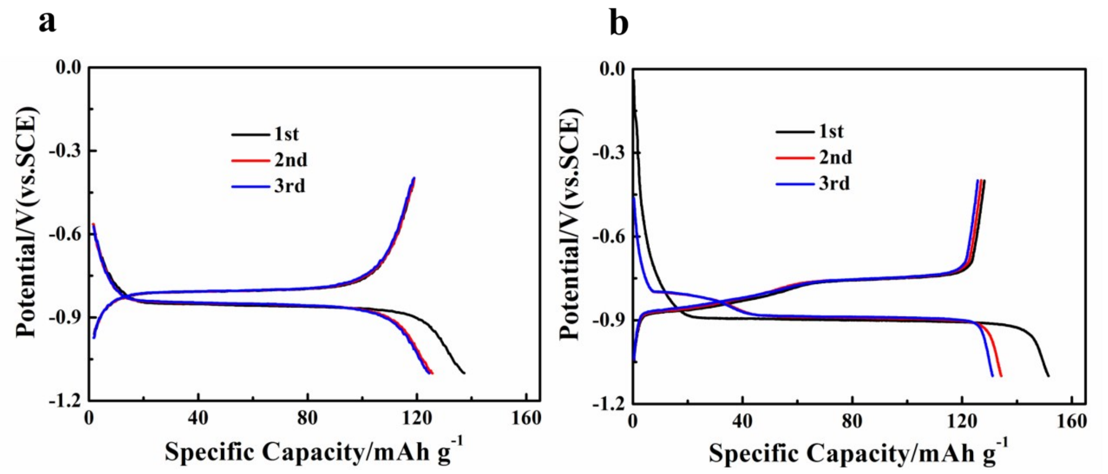

Figure S2. (a)The charge/discharge profiles of NTP@C electrode in 2 M Na_2SO_4 solution, the current rate is 1 C, 1 C=150 mA g^{-1}; (b) The charge/discharge profiles of NTP@C electrode in 2 M Li_2SO_4 solution, the current rate is 1 C, 1 C=150 mA g^{-1}.

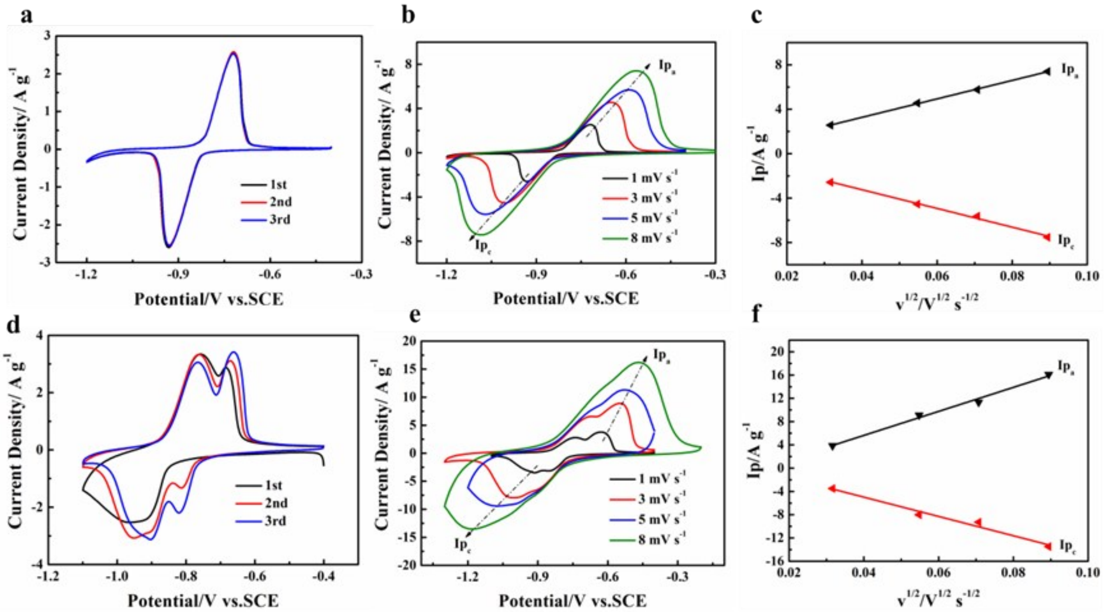

Figure S3. (a)The CV profiles of NTP@C electrode in 2 M Na_2SO_4 solution, the scanning rate is 1 mV s^{-1}; (b) The CV profiles of NTP@C electrode in 2 M Na_2SO_4 solution, the scanning rate is from 1 mV s^{-1} to 8 mV s^{-1}; (c) The fitting lines of the Ip and v$^{1/2}$ (NTP@C electrode in 2 M Na_2SO_4 solution); (d) The CV profiles of NTP@C electrode in 2 M Li_2SO_4 solution, the scanning rate is 1 mV s^{-1}; (e) The CV profiles of NTP@C electrode in 2 M Li_2SO_4 solution, the scanning rate is from 1 mV s^{-1} to 8 mV s^{-1}; (f) The fitting lines of the Ip and v$^{1/2}$ (NTP@C electrode in 2 M Li_2SO_4

solution);

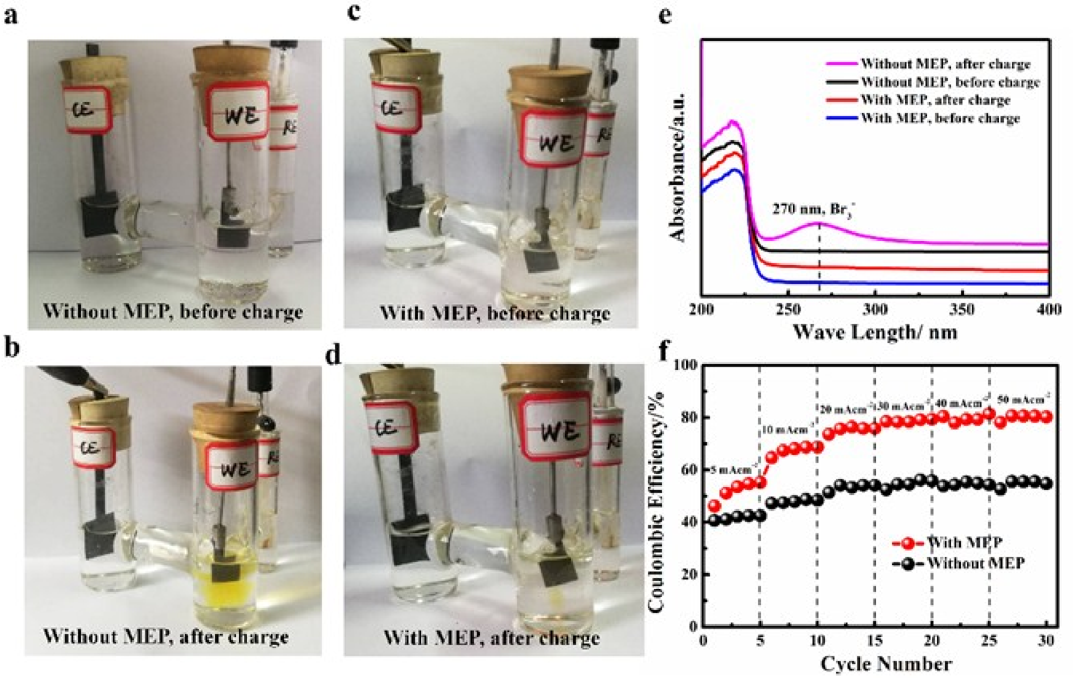

Figure S4. Results of three-electrode tests of Br_3^-/Br^- redox pair when with or without MEP in electrolyte. (a) before charge when without MEP; (b) after charge for 1 mA h at a current density of 5 mA cm^{-2} when without MEP; (c) before charge when with MEP; (d) after charge for 1 mA h at a current density of 5 mA cm^{-2} when with MEP; (e) UV-Vis spectra of the bulk solution before and after charge; (f) comparison of coulombic efficiencies when with or without MEP.

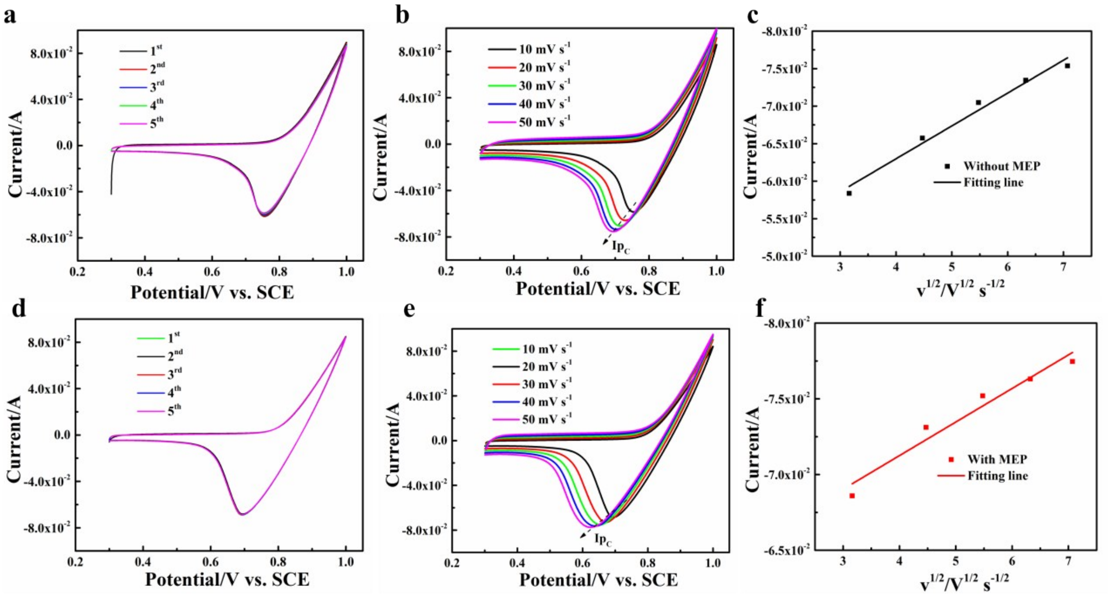

Figure S5. (a)The CV profiles of bromine catholyte without MEP additive, the scanning rate is 10 mV s^{-1}; (b) The CV profiles of bromine catholyte without MEP additive, the scanning rate is from 10 mV s^{-1} to 50 mV s^{-1}; (c) The fitting lines of the Ip and $v^{1/2}$ (bromine catholyte without MEP additive); (d) The CV profiles of bromine catholyte with MEP additive, the scanning rate is 10 mV s^{-1}; (e) The CV profiles of bromine catholyte with MEP additive, the scanning rate is from 10 mV s^{-1} to 50 mV s^{-1}; (f) The fitting lines of the Ip and $v^{1/2}$ (bromine catholyte with MEP additive);

Table S1. The kinetic parameters of bromine catholyte with or without MEP additive.

Bromine or NTP@C	D(cm^2 s^{-1})/(cm^2 s^{-1})CV
With MEP	$1.40*10^{-5}$
Without MEP	$3.62*10^{-6}$
NTP@C	$1.25 *10^{-8}$

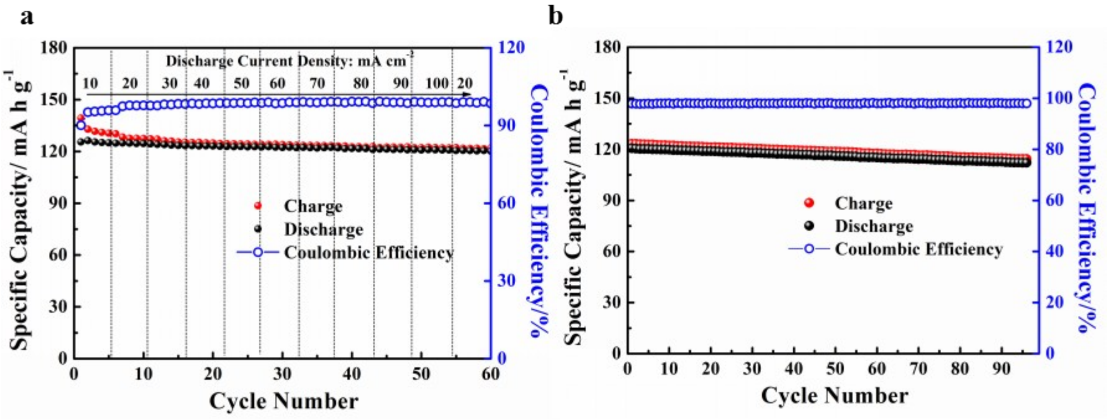

Figure S6. (a) The discharge capacities Br-NTP-D-MEP-Na (using Na^+ solution, based on the mass of negative active material) of these batteries under different current densities; (b) The cycling performance under 20 mA cm^{-2}.

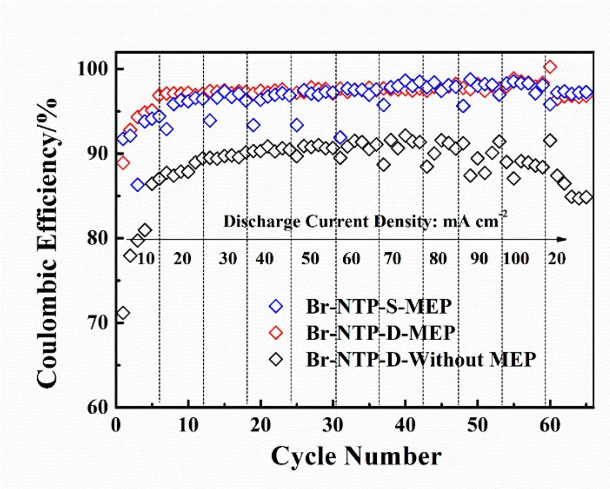

Figure S7. Comparison of the coulombic efficiencies of three batteries at different current densities.

Table S2. pH values of various electrolytes

pH Battery/ Electrolyte	Before/After charging Positive electrolyte	 Negative electrolyte
Br-NTP-S-MEP	7.9/3.8	7.9/6.0
Br-NTP-D-MEP	7.9/3.8	7.9/6.1
Br-NTP-D-Without MEP	7.9/3.5	7.9/5.5

The pH values of batteries before and after 200 cycles were recorded and summarized in Table S2. The initial pH values of the catholyte and negative electrolyte are similar and both around 8.0, which is still mild and near neutral. The pH value of negative electrolytes is around 6.0 after 200 cycles. As reported, the phosphate materials will become less stable in aqueous electrolyte at pH > 9 or pH < 4, which are obviously yet reached in the negative electrolyte. However, the pH environment of catholytes becomes more acid (pH value is near 4.0). The disproportionation of Br_2 (Br_2+H_2O == HBr+HBrO) and decomposition of H_2O (H_2O==O_2+H^+) are the two possible reasons. Though acid environment is hazard to the structure stability of ion intercalation cathode materials, it is still suitable to keep the high reactivity of Br^-/Br_2 redox reaction. Therefore, we think that the pH value indeed changes during the cycling process, but it shows less effect on the electrochemical performance of hybrid batteries.

Table S2. Comparison of various aqueous ion batteries.

Battery (cathode//anode)	Voltage/ V	Mass loading/ mg cm^{-2}	Current density/ mA cm^{-2}	Actual capacity/ mA h cm^{-2}	Ref.
B_3^-/Br^-//NTP	1.47	80	20	8.7	This work
		80	50	8.2	
		80	100	7.2	
$Fe(CN)_6$//$Fe(CN)_6$	0.7	4	0.85	0.168	1
		4	2.12	0.164	
		4	4.25	0.144	
		4	8.5	0.1	
$NaMnO_2$//NTP	1.15	2.5	0.15	0.24	2
		2.5	1.5	0.17	
		2.5	3	0.15	
$LiMn_2O_4$//NTP	1.48/1.6	6	0.03	0.115	3
		6	0.15	0.11	
		6	1.5	0.083	
$Na_{0.44}MnO_2$//NTP	1.1	40	1.064	4.84	4
		40	10.64	4.12	
		40	26.6	2.72	
$LiMn_2O_4$//LTP	1.50	10	2.76	1.172	5
		10	27.6	1.042	
		10	55.2	0.86	
$LiMn_2O_4$//PI-AC	1.21	3	1.8	0.252	6
$LiMn_2O_4$//LTP@C-N	1.48/1.6	6	0.9	0.738	7
		6	3.6	0.672	
		6	9	0.618	
NVPF//NTP	1.5	2.7	2.88	0.142	8

$Na_{0.44}MnO_2$//NTP	1.1	17.6	4.8	1.83	9
		17.6	14.4	1.79	
		17.6	96	1.56	
$LiMn_2O_4$//Zn	1.8/2.0	6	0.18	0.72	10
		6	0.72	0.579	
$LiMn_2O_4$//$PbSO_4$	1.3	3.75	1.5	0.44	11
			7.5	0.35	
			11.3	0.29	

Reference:

1. J. Zhang, D. Zhang, F. Niu, X. Li, C. Wang and J. Yang, *ChemPlusChem*, 2017, **82**, 1170-1173.
2. Z. Hou, X. Li, J. Liang, Y. Zhu and Y. Qian, *J. Mater. Chem. A*, 2015, **3**, 1400-1404.
3. D. Sun, G. Jin, Y. Tang, R. Zhang, X. Xue, X. Huang, H. Chu and H. Wang, *Journal of The Electrochemical Society*, 2016, **163**, A1388-A1393.
4. W. Wu, S. Shabhag, J. Chang, A. Rutt and J. F. Whitacre, *Journal of the Electrochemical Society*, 2015, **162**, A803-A808.
5. H. Wang, H. Zhang, Y. Cheng, K. Feng, X. Li and H. Zhang, *Journal of Materials Chemistry A*, 2017, **5**, 593-599.
6. Z. Guo, L. Chen, Y. Wang, C. Wang and Y. Xia, *ACS Sustainable Chemistry & Engineering*, 2017, **5**, 1503-1508.
7. D. Sun, X. Xue, Y. Tang, Y. Jing, B. Huang, Y. Ren, Y. Yao, H. Wang and G. Cao, *ACS applied materials & interfaces*, 2015, **7**, 28337-28345.
8. P. R. Kumar, Y. H. Jung, B. Moorthy and D. K. Kim, *Journal of The Electrochemical Society*, 2016, **163**, A1484-A1492.
9. Z. Li, D. Young, K. Xiang, W. C. Carter and Y.-M. Chiang, *Advanced Energy Materials*, 2013, **3**, 290-294.
10. T. K. A. Hoang, T. N. L. Doan, C. Lu, M. Ghaznavi, H. Zhao and P. Chen, *ACS Sustainable Chemistry & Engineering*, 2016, **5**, 1804-1811.
11. Y. Liu, Z. Wen, X. Wu, X. Wang, Y. Wu and R. Holze, *Chemical communications*, 2014, **50**, 13714-13717.